

## Selective Oxidation of Methane to Methanol on Dispersed Copper on Alumina from Readily Available Copper(II) Formate.

Jordan Meyet, Alexander P. van Bavel, Andrew D. Horton, Jeroen A. van Bokhoven\*, Christophe Copéret\*

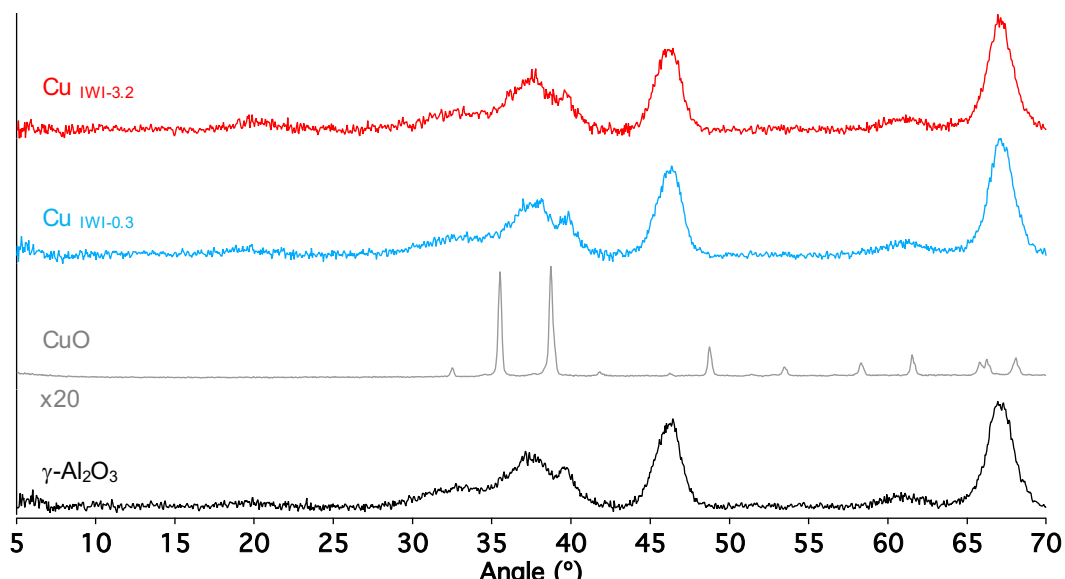


Figure S1: Powder XRD of  $\gamma\text{-Al}_2\text{O}_3$  (black), CuO (gray),  $\gamma\text{-Al}_2\text{O}_3$  after impregnation of 0.3 wt% Cu (blue) and 3.2 wt% Cu (red)

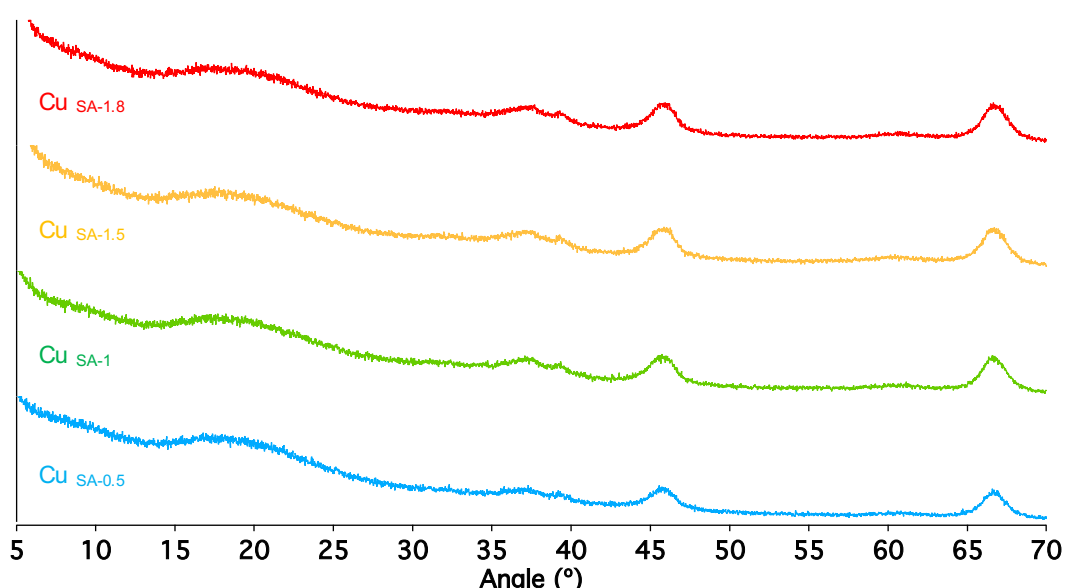


Figure S2: Powder XRD of  $\gamma\text{-Al}_2\text{O}_3$  after specific adsorption of 0.5 wt% Cu (blue), 1.0 wt% Cu (green), 1.5 wt% Cu (orange) and 1.8 wt% Cu (red)

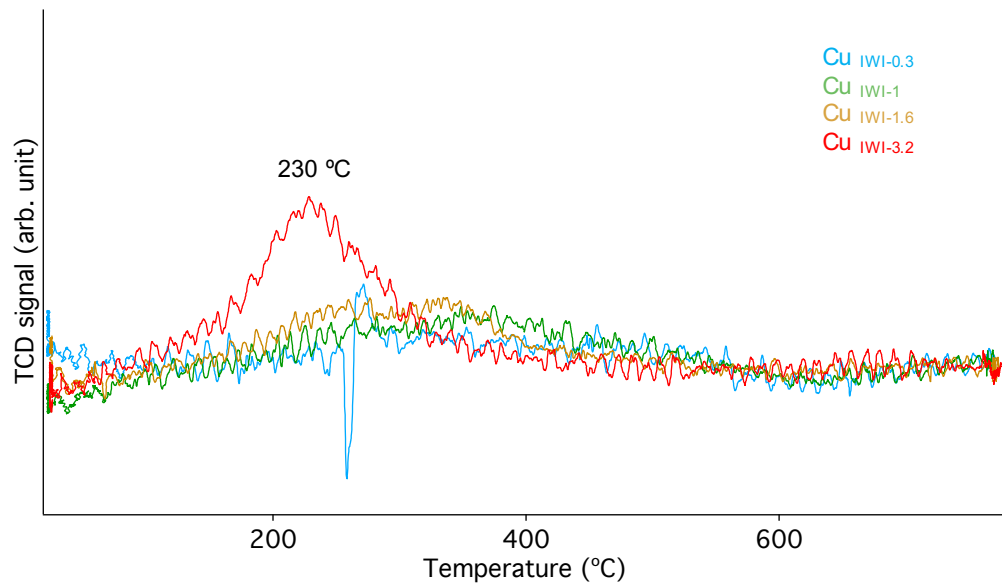


Figure S3: Temperature programmed reduction (TPR) of the incipient wetness impregnation samples after activation at 500 °C under synthetic air

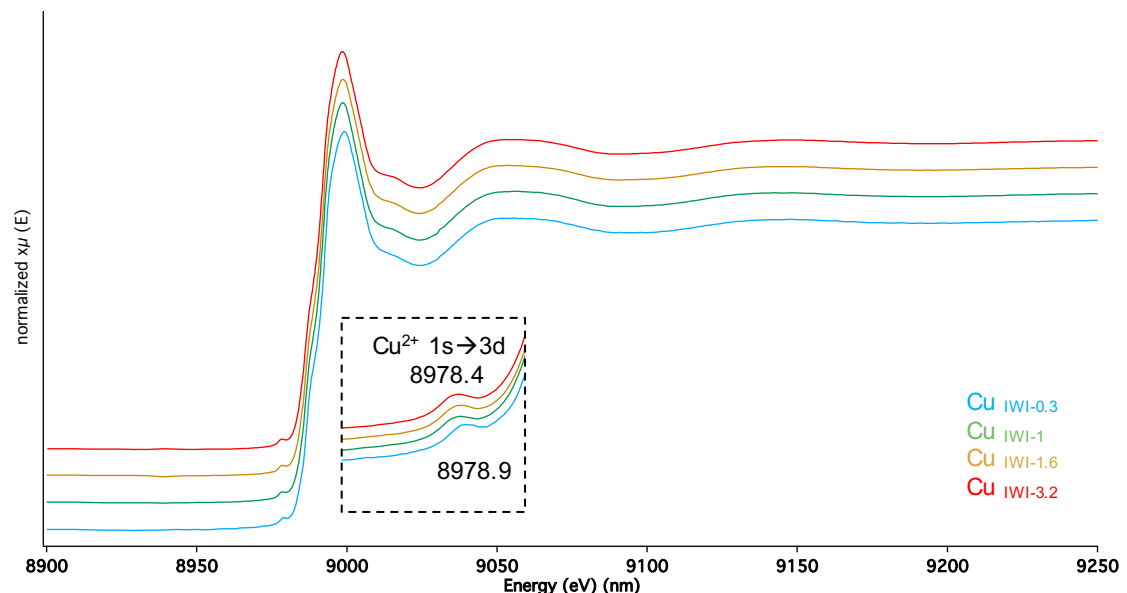


Figure S4: Cu K-edge X-Ray Adsorption Near Edge (XANES) spectroscopy of  $\gamma\text{-Al}_2\text{O}_3$  prepared by IWI after calcination at 500 °C

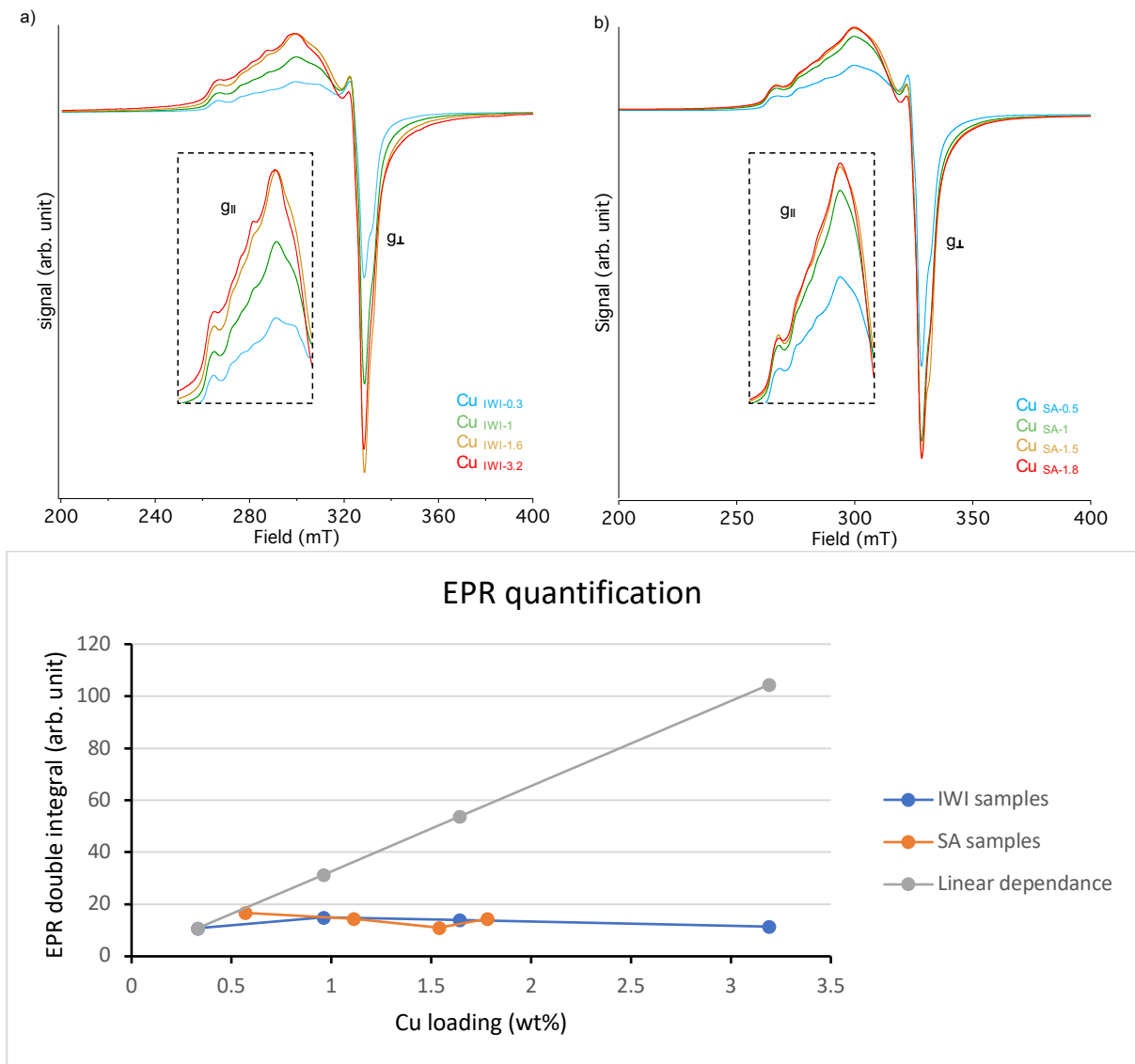


Figure S5: X-band CW-EPR spectra of the IWI (a) and SA (b) samples after activation at 500 °C under synthetic air

Material	loading	Site density	$\text{CH}_3\text{OH}$ yield	$\text{CH}_3\text{OH}$ yield	EPR quantification
IWI	wt% Cu	Cu.nm <sup>-1</sup>	$\mu\text{mol.g}^{-1}$	mol $\text{CH}_3\text{OH} \cdot \text{mol}^{-1} \text{Cu}$ (%)	$\text{Cu}^{2+}$ reduced (%)
<b>Cu</b> IWI-0.3	0.33	0.1	3.0	5.8	10.8
	0.96	0.4	6.8	4.5	15
	1.64	0.7	11.8	4.6	13.9
	3.19	1.3	14.4	2.9	11.5
	<b>Cu</b> IWI-0.3	0.33	0.1	4.4	n.d
	<b>Cu</b> IWI-1	0.75	0.3	6.9	n.d
	<b>Cu</b> IWI-1.6	1.68	0.7	11.6	n.d
	<b>Cu</b> IWI-3.2	2.89	1.2	14.8	n.d
<b>SA</b>					
<b>Cu</b> SA-0.5	0.57	0.2	5.2	5.9	16.7
	1.11	0.5	7.9	4.5	14.5
	1.54	0.6	8.2	3.4	11
	<b>Cu</b> SA-1.8	1.78	0.7	21.0	14.5

Table S1: Reactivity summary for the IWI and SA samples for the partial oxidation of methane to methanol

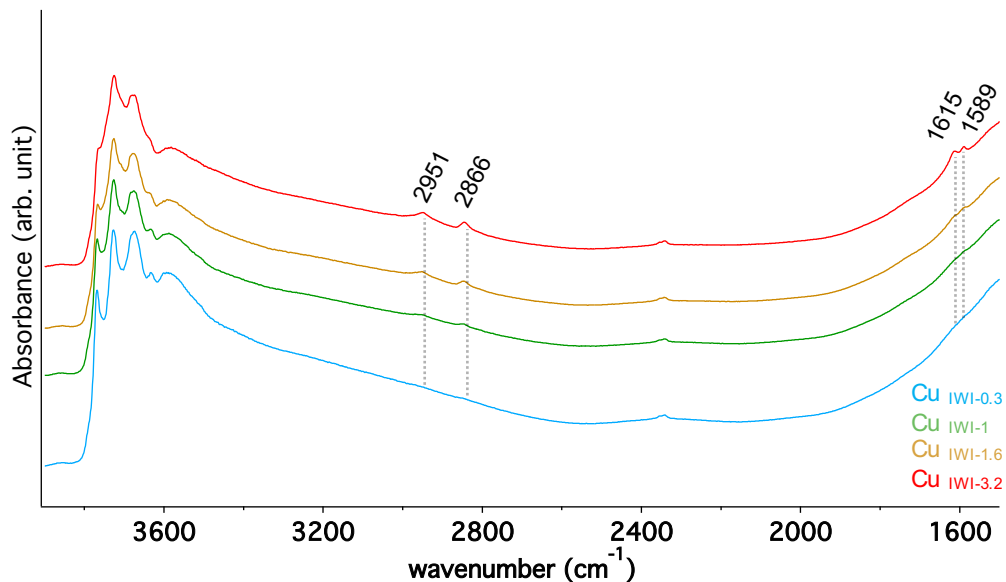


Figure S6: DRIFT spectra of the incipient wetness impregnation samples after reaction with  $\text{CH}_4$  (6 bar, 200 °C, 30 min)

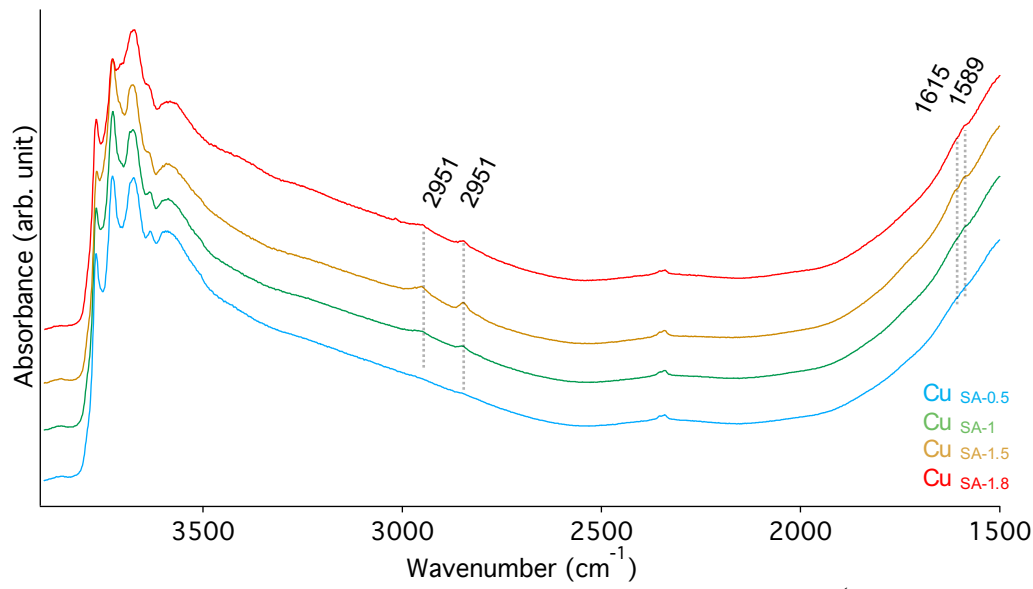


Figure S7: DRIFT spectra of the specific adsorption samples after reaction with CH<sub>4</sub> (6 bar, 200 °C, 30 min)

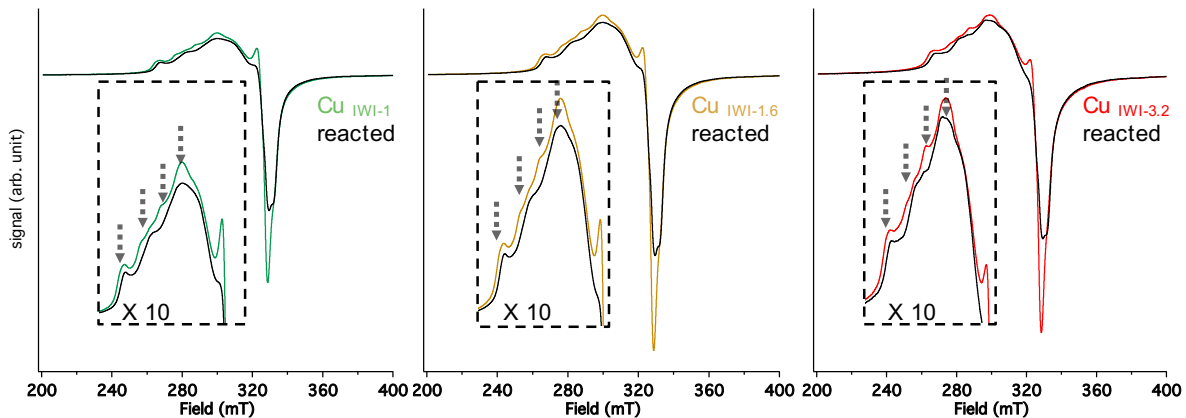


Figure S8: In situ X-band CW-EPR spectra at 25 °C of the incipient wetness impregnation series before (colored) and after (black) reaction with 6 bar of CH<sub>4</sub> at 200 °C for 30 min. The insert shows a magnification of the parallel transition region and the grey arrows indicate the Cu hyperfine coupling that decrease after reaction with CH<sub>4</sub>.

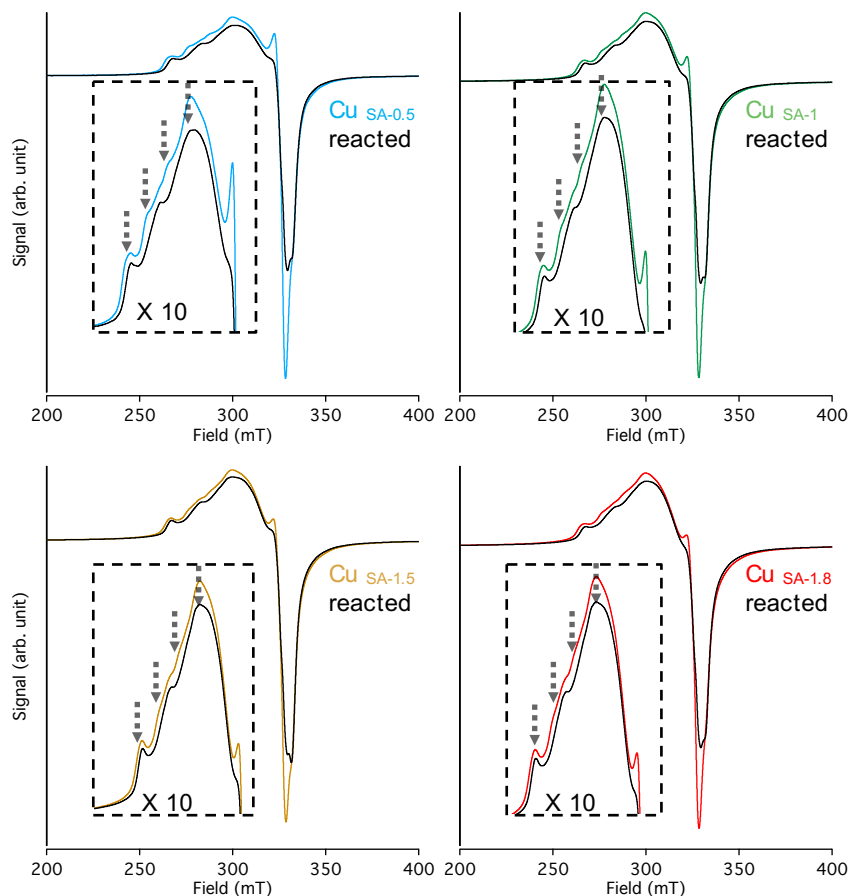


Figure S9: *In situ* X-band CW-EPR spectra at 25 °C of the specific adsorption series before (colored) and after (black) reaction with 6 bar of CH<sub>4</sub> at 200 °C for 30 min. The insert shows a magnification of the parallel transition region and the grey arrows indicate the Cu hyperfine coupling that decrease after reaction with CH<sub>4</sub>.

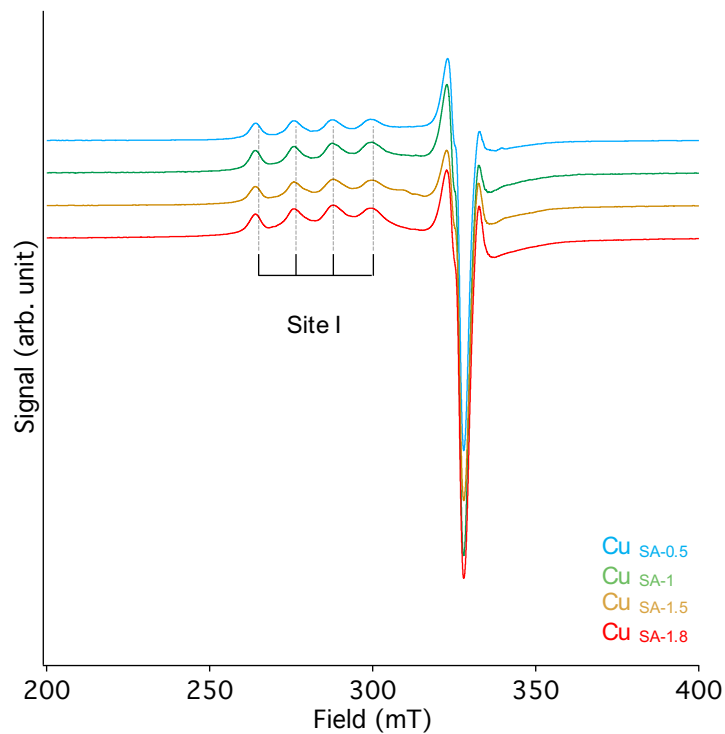


Figure S10: Resulting difference spectra for the specific adsorption series showing the same spectral signature of the monomeric Cu<sup>2+</sup> active site in all samples.

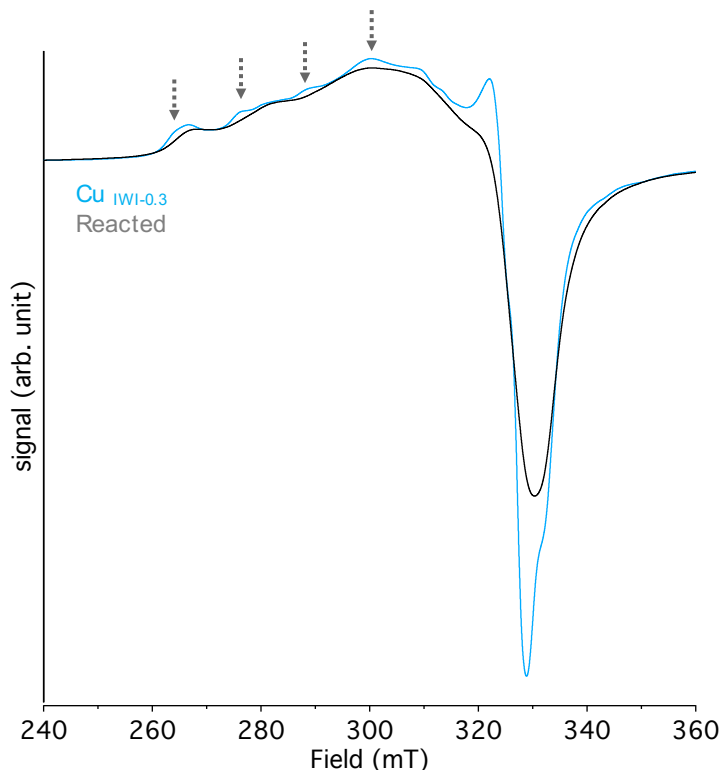


Figure S11: X-Band EPR spectrum ( $-170^{\circ}\text{C}$ ) for Cu<sub>IWI-0.3</sub> before and after reaction under 6 bar of CH<sub>4</sub> for 30 min at  $200^{\circ}\text{C}$ . The grey arrows indicates the Cu hyperfine coupling that decrease after reaction with CH<sub>4</sub>.

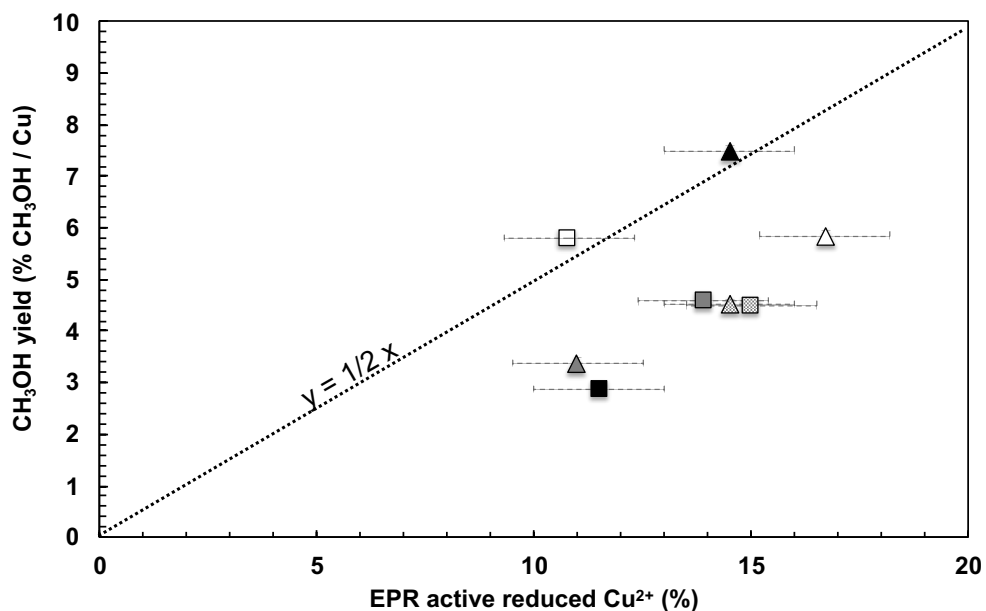


Figure S12: Correlation of the methanol yield in mol% CH<sub>3</sub>OH. mol%<sup>-1</sup> Cu with the reduced Cu<sup>2+</sup> species probed by EPR. IWI samples (■) and SA samples (▲). Grey scale measure for loading with white being the lowest one and black the highest one. The error bar for the reduced Cu<sup>2+</sup> was determined experimentally by performing the reaction *in situ* under argon atmosphere with Cu<sub>IWI-1.6</sub> and calculated to be 3%.